Case Studies in Mechanical Systems and Signal Processing 1 (2015) 15–26

Contents lists available at ScienceDirect

Case Studies in Mechanical Systems and Signal Processing

journal homepage: www.elsevier.com/locate/csmssp

Case Study

Rotor failure detection of induction motors by wavelet transform and Fourier transform in non-stationary condition

Cesar da Costa [a,*], Masamori Kashiwagi [b], Mauro Hugo Mathias [b]

[a] Electrotechnical Engineering, IFSP – Federal Institute of Education, SP 01109-010, Brazil
[b] Mechanical Engineering, UNESP – Universidade Estadual Paulista, SP 12516-410, Brazil

ARTICLE INFO

Article history:
Received 18 November 2014
Received in revised form 13 May 2015
Accepted 13 May 2015
Available online 15 June 2015

Keywords:
Rotating electrical machine
Diagnostic
Digital signal processing

ABSTRACT

This case study presents two diagnostic methods for the detection of broken bars in induction motors with squirrel-cage type rotors: FFT method and wavelet method. The FFT method allows detecting broken rotor bar when the motor operates under a load, but if the machine is decoupled from the mechanical load, the side band components associated with broken bars do not appear. The WT is a powerful signal-processing tool used in power systems and other areas. New wavelet-based detection methods that are focused on the analysis of the startup current have been proposed for the detection of broken bars. Since the transient stator current signal is not periodic, it is not amenable to analyze the signal by FFT method. In addition, it is impossible to estimate the time of the fault occurrence using the FFT. In this paper, our main goal is to find out the advantages of wavelet transform method compared to Fourier transform method in rotor failure detection of induction motors.

1. Introduction

Induction motors with a squirrel-cage rotor are widely used in many industrial processes, and they play important roles in various processing industries [1,2]. Despite their low cost, from the reliability and robustness viewpoint, induction motors are prone to failure owing to their exposure to a variety of harsh environments and incorrect operating conditions or manufacturing defects. If not identified in time, these failures and gradual deterioration can lead to motor disruption and increase in electricity consumption. It is known that early fault detection of induction machines can not only minimize damage and reduce energy consumption but also prevent the spread of failure or limit its escalation in terms of severity. Therefore, diagnostic or engine condition monitoring systems received considerable attention over the past 10 years [3,4]. Failure of the bars of squirrel-cage rotors rarely causes immediate failure, especially in large multi-pole motors (slow speed). However, if a sufficient number of rotor bars are broken, the motor cannot start because it cannot develop sufficient torque. Breakage of broken bar occurs in large induction motors (Fig. 1), which have rather long startup time, and the fault must be detected during the startup time. This is much important when the problem such as intensive unbalanced magnetic

* Corresponding author. Tel.: +55 1132535693.
E-mail addresses: cost036@attglobal.net (C. da Costa), masamorika@uol.com.br (M. Kashiwagi), mathias@feg.unesp.br (M.H. Mathias).

http://dx.doi.org/10.1016/j.csmssp.2015.05.001

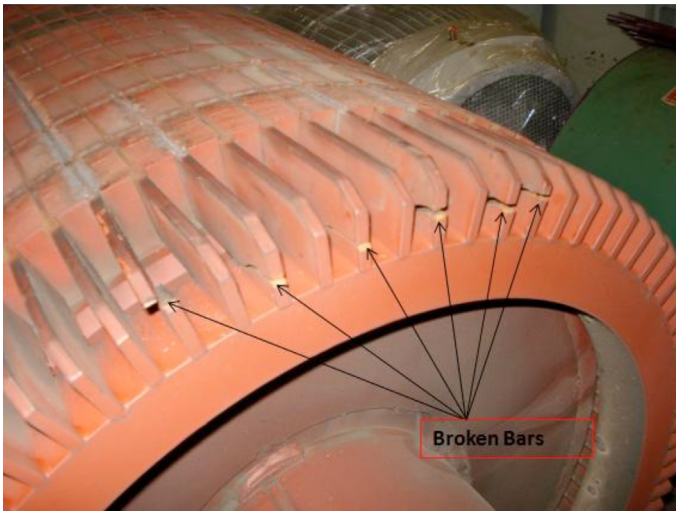

Fig. 1. Squirrel-cage rotor with 6 broken bars of a large induction motor.

pull and even arcing during the startup of the motor under the fault exist. One of the purposes of this case study is presenting a fault detection method and determination of the broken bars during the startup time.

This paper is organized as follows. Section 2 gives a brief description of Fourier transform and wavelet transform. Section 3 presents the spectral analysis method. Section 4 presents wavelet analysis method. Section 5 presents the experimental setup and results with FFT and wavelet method. Finally, Section 6 presents the conclusion.

2. Fourier transform (FT) versus wavelet transform

The FFT-based method such as MCSA cannot provide a tool to diagnose the fault during startup. The reason is FFT processor is applicable in static (steady) signals and it cannot be used to analyze the transient of the motor in which both amplitude and frequency vary. One of the difficulties existing in the fault detection is the precise detection of the fault in induction motor with varying load. For instance, the FFT-based MCSA method which uses side-band components around fundamental harmonic to detect the fault, suffers from this difficulty. The reason is the amplitude of the side-band components is load-dependent; therefore, it is possible to diagnose the fault by comparison of the amplitude of the side band around the fundamental harmonic in healthy and faulty motor for an identical load in both cases. A simple approach is to move a short time window along the signal obtain the Fourier spectrum as a function of time shift. This is called the short time Fourier transform (STFT). Even so, the STFT is sometimes useful for tracking changes in frequency with time, even with the restriction of resolution [5,12].

The problem here is that the system is based on the short-time Fourier transform. The transform divides a non-stationary signal into small windows of equal time. The Fourier transform is then applied to the time segment being examined. As the width or support of the window function decreases, a smaller portion of the input signal is considered, guaranteeing a greater time localization of frequency components in the signal. As the support of the window function increases, more accurate information about frequencies within the window is increased, but the ability to determine the time when those transients occur within the input signal is lost.

Using wavelets can solve the above-mentioned problems and a more precise behavior of the stator current signal can be described [5–7]. The WT is a powerful signal processing tool used in power systems and other areas. The WT, like the STFT, allows time localization of different frequency components of a given signal, however, with one important difference: the STFT uses a fixed width windowing function. As a result, both frequency and time resolution of the resulting transform will be fixed but in the case of the WT, the analyzing functions, which are called wavelets, will adjust their time widths to their frequency in such a way that higher frequency wavelets will be very narrow and lower frequency ones will be broader. Therefore, in contrast to the STFT, the WT can isolate the transient components in the upper frequency isolated in a shorter part of power frequency cycle. The ability of the WT to focus on short time intervals for high frequency components and long intervals for low-frequency components improves the analysis of the signals with localized impulses and oscillations [8,12].

3. Spectral analysis

The frequency spectrum of a signal is basically the frequency components (spectral components) of that signal. The frequency spectrum of a signal shows what frequencies exist in the signal. Spectral analysis refers to the representation of

current signals in the frequency domain. The Fourier transform (FT) defines that a periodic waveform in the time domain can be represented by a weighted sum of sines and cosines. The same waveform can then be represented in the frequency domain as an amplitude–phase pair for each frequency component.

Spectral analysis of stator current using the fast Fourier transform (FFT) is applied to the detection of broken rotor bars. According to [1,5], in a three-phase induction motor with a squirrel-cage rotor, the rotor bars break or crack in the rotor ring termination bars, disturb the magnetic flux, the rotor frequency, thus, altering the spectrum of stator current.

Several works such as [1,5,6] have used fast Fourier transform (FFT) for spectral analysis of stator current to diagnose broken rotor bars. From these works, internal faults of broken rotor bars may be detected in the stator current spectrum.

3.1. Current signal processing

In the normal operation of an induction motor, frequency of the rotor induced current is equal to sf_0. Here, f_0 is the supply frequency and s is the slip $s = (n_s - n)/n_s$; n_s is a constant (synchronous speed) and n is machine speed. This current generates a forward field with the speed with respect to the rotor. If the rotor has a broken bar, the rotor current with frequency sf_0 consists of two forward and backward components that generate the fields with speeds $\pm sf_0$ with respect to the rotor.

The forward traveling wave represents the main magnetic field and the backward traveling wave is due to the electrical rotor asymmetry. For infinite inertia drives the backward traveling wave induces a stator voltage harmonic component at the frequency [5,6]:

$$f_{lsb} = (1 - 2s) f_0 \tag{1}$$

The impedance of the machine (including supply) leads to a stator current harmonic with the same frequency as the induced stator voltage harmonic. Since the frequency of this harmonic component is less than the frequency of the fundamental wave this stator current harmonic component is called the *lower side band* harmonic. A finite inertia of the drive causes an additional *upper side band* harmonic current at frequency [5,6]:

$$f_{usb} = (1 + 2s) f_0 \tag{2}$$

Due to the interaction of these side band currents with flux and the inertia specific speed ripple, additional harmonics arise:

$$f_{lsb}[k] = (1 - 2ks) f_0 \tag{3}$$

$$f_{usb}[k] = (1 + 2ks) f_0 \tag{4}$$

where k is an integer order number. Between no load and rated operating conditions slip s varies between zero and some percent. The side band currents of stator currents are also reflected in the flux linkages of the main field (air gap) and the stray flux. There is therefore a cyclic variation of stator current that causes a torque pulsation at twice slip frequency ($2sf_0$) and a corresponding speed oscillation that is also a function of the drive inertia. This speed oscillation can reduce the magnitude of the $(1 - 2s) f_0$ sideband, but an upper sideband current component at $(1 + 2s) f_0$ is induced in the stator winding due to the rotor oscillation [6]. This upper sideband is also enhanced by the third harmonic of the flux. Broken rotor bars therefore result in current components being induced in the stator winding at frequencies given by:

$$f_{bb} = (1 \pm 2s) f_0 \tag{5}$$

The most common rotor fault detection methods are based on the measurement of the stator current on steady-state current. This class of methods are called motor current signature analysis (MCSA) methods. Then a fast Fourier transform (FFT) [6] is performed in order to determine the fault specific current harmonic side bands. Fig. 2(a) shows spectrum of stator current for a loaded healthy motor and Fig. 2(b) shows spectrum of stator current for loaded motor with one broken bar.

4. Wavelet analysis

Wavelet transform has been applied in various branches of science owing to their peculiar characteristic of detailing signal specific points [9–13]. In applications where very-high-precision frequency analysis is required as on transient current, the traditional fast Fourier transform method does not yield satisfactory results and does not possess the ability to drill regions of interest in the signal. In terms of methods for detecting broken bars in a squirrel-cage rotor, wavelets, which use the startup current of the motor, are very effective. During motor startup, the speed varies from zero to near synchronous speed. More recent examples regarding the application of wavelets to detection of the motor condition can be found in [14–21].

4.1. Theoretical of wavelets method

The continuous wavelet transform (CWT) was developed as an alternative approach to the STFT to overcome its resolution problem. The wavelet analysis is done in a similar way to the STFT analysis, in the sense that the signal is

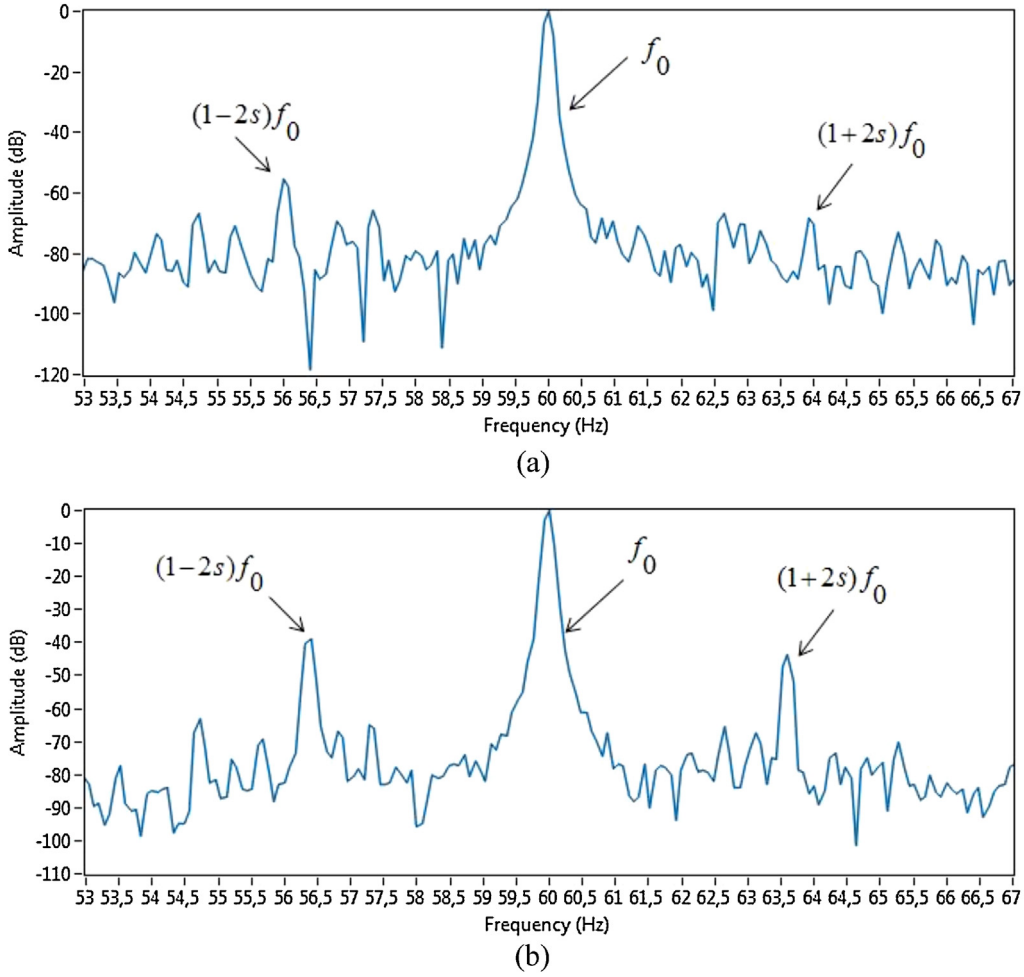

Fig. 2. Spectrum of stator current for (a) loaded healthy motor; (b) loaded motor with one broken bar.

multiplied with a function, with the wavelet, similar to the window function in the STFT, and the transform is computed separately for different segments of the time-domain signal. The continuous wavelet transform is defined by the following equation:

$$W(a,b) = \frac{1}{\sqrt{a}} \int_{-\infty}^{\infty} x(t)\psi^* \left(\frac{(t-b)}{a} dt \right) \tag{6}$$

As it can be seen the transformed signal is a function of two variables (b and a, the translation and scale parameters), respectively $\psi(t)$ is the transforming function, and it is called the mother wavelet, a prototype for generating the other window functions. The term translation is used in the same sense as it was used in the STFT; it is related to the location of the window, as the window is shifted through the signal. This term, obviously, corresponds to time information in the transform domain. The parameter scale in the wavelet analysis is similar to the scale used in maps. High scales correspond to a non-detailed global view (of the signal), and low scales correspond to a detailed view. Similarly, in terms of frequency, low frequencies (high scales) correspond to a global information of a signal, whereas high frequencies (low scales) correspond to a detailed information of a hidden pattern in the signal (that usually lasts a relatively short time).

Once the mother wavelet is chosen the CWT computation starts with $a = 1$. The wavelet at this scale then is shifted toward the right by b amount to the location $t = b$, and Eq. (6) is computed to get the transform value at $t = b$, $a = 1$ in the time–frequency plane. This procedure is repeated until the wavelet reaches the end of the signal. One row of points on the time-scale plane for the scale $a = 1$ is now completed. In this way the continuous wavelet transform is computed for all the imposed values of a.

For the discrete wavelet transform (DWT) the main idea is the same as it is in the case of CWT, but it is considerably easier and faster to implement. A time-scale representation of a digital signal can be obtained using digital filtering techniques. Filters of different cutoff frequencies are used to analyze the signal at different scales. The signal is passed through a series of high pass filters to analyze the high frequencies, and it is passed through a series of low pass filters to analyze the low frequencies.

The DWT analyses the signal at different frequency bands with different resolutions by decomposing the signal into a coarse approximation and detail information. DWT employs two sets of functions, called scaling functions and wavelet functions, which are associated with low pass and highpass filters, respectively. According to [5,12,13], with multi-resolution analysis (MRA), a wavelet-based technique, a signal S can be decomposed and reconstructed by means of two components: approximation (a_1) and detail (d_1), where approximation can be interpreted as a high-pass filter and detail as a low-pass filter. This means that the approximation contains the low-frequency information of the original signal and detail contains the high-frequency information. The decomposition of the signal into different frequency bands (Fig. 3) is simply obtained by successive highpass and lowpass filtering of the time domain signal.

4.2. Detection of side band by wavelets method

According to [20], the level-n DWT decomposition of a sampled signal $i_s = (i_1, i_2, i_3, \ldots, i_q)$ consists of a digital filtering process with $n+1$ stages. The signal is passed through n high-pass filters and low-pass filters. Resulting from this multiple filtering process, n vectors of detail coefficients $\beta^j = \beta_i^j$ (j = decomposition level) and a vector of approximation coefficient $\alpha^n = \alpha_i^n$ are obtained. Actually, the process for obtaining the DWT is made by using a recursive algorithm of high computational efficiency denominated as ''Mallat's algorithm'' or pyramidal algorithm. From these coefficients, the signal can be reconstructed by using the inverse transform. The reconstructed signal consists of the sum of n detail signals (d) and an approximation signal (a); each one containing the same number of samples q as the original signal:

$$i_s(t) = d_1 + d_2 + \cdots + d_n + a_n \tag{7}$$

If a bar breakage exists, the left sideband harmonic has a significant amplitude throughout the startup process; because its frequency is always below f_0, it causes a significant increase in the energy of the approximation signal a_{nf} during the startup process [20].

Therefore, the decomposition level of the approximation signal that includes the left sideband harmonic is given by the following:

$$n_f = \text{integer}\left[\frac{\log(f_s/f_0)}{\log(2)}\right] \tag{8}$$

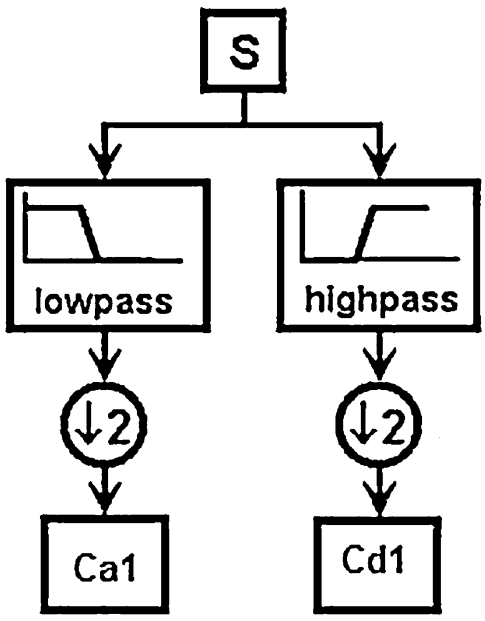

Fig. 3. The DWT decomposition of a signal.

The value of the decomposition level depends on the sampling frequency (f_s), and this can be easily calculated from Eq. (9) that specifies that the upper limit of the frequency interval of a_{nf} is lower than the supply frequency [15–20]:

$$2^{-(n_f+1)} \cdot f_s < f_0 \tag{9}$$

5. Experimental set up

For validating the motor condition monitoring method by FFT, several tests were performed with a 4-pole, 3-phase, 60 Hz, 1.5 kW, 220/380 V (rated voltage), 1750 rpm (rated speed), and 28-rotor-bar induction motor. Fig. 4 shows the experimental setup. The load was a 2 kW DC machine with a rated speed of 1800 rpm. To demonstrate the application of the fault detection by FFT method, we performed an analysis of different signals collected from rotor broken bars was performed. The broken bars were artificially manufactured in the laboratory by opening the motor and drilling holes in different bars.

5.1. Experimental results with FFT method

Several tests under different loads for healthy rotors and faulty rotors with broken bars were performed on steady-state. In each case, the stator current was transformed in the frequency domain and analyzed by the FFT method. The sampling rate defined was 2 kHz, 4000 samples and frequency resolution equal 0.5 Hz. Then, the fault frequency components of the f_{lsb} (lower side band) is equal 56 Hz $(1-2s)\,f_0$) and f_{usb} (upper side band) is equal 64 Hz $((1+2s)f_0)$ are analyzed. Fig. 5 shows

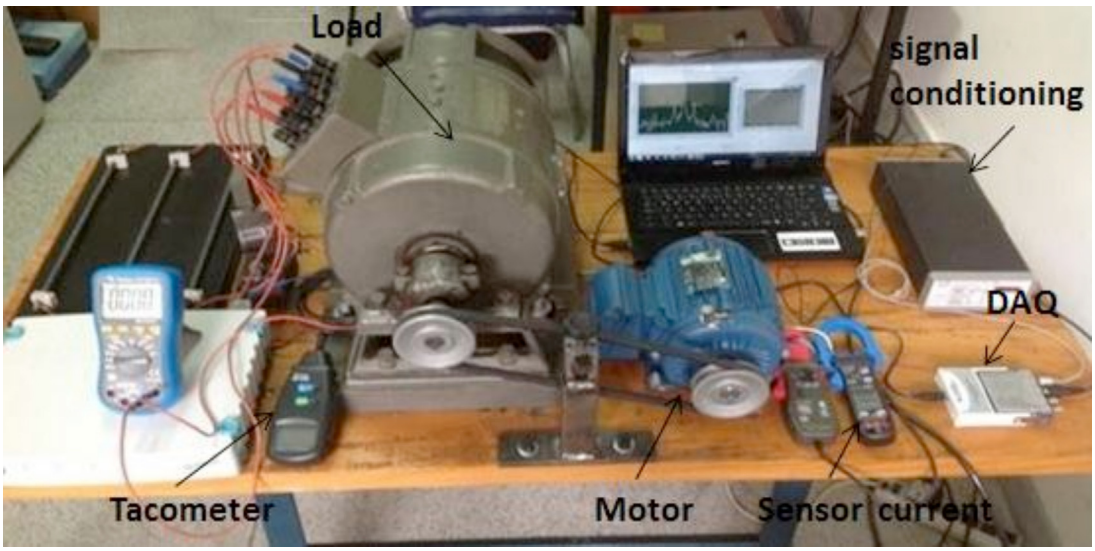

Fig. 4. Experimental set up for (a) 1.5 kW motor; (b) rotor bar breakages.

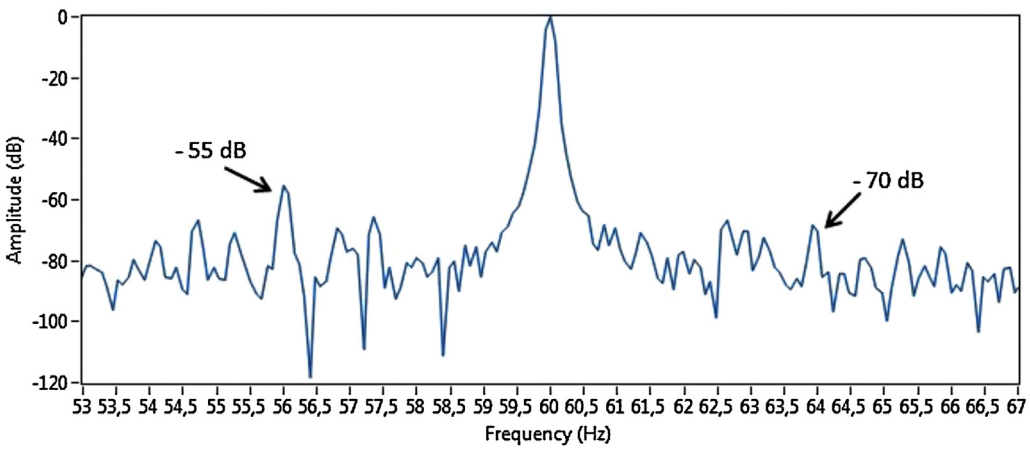

Fig. 5. Spectrum of stator current for loaded healthy motor.

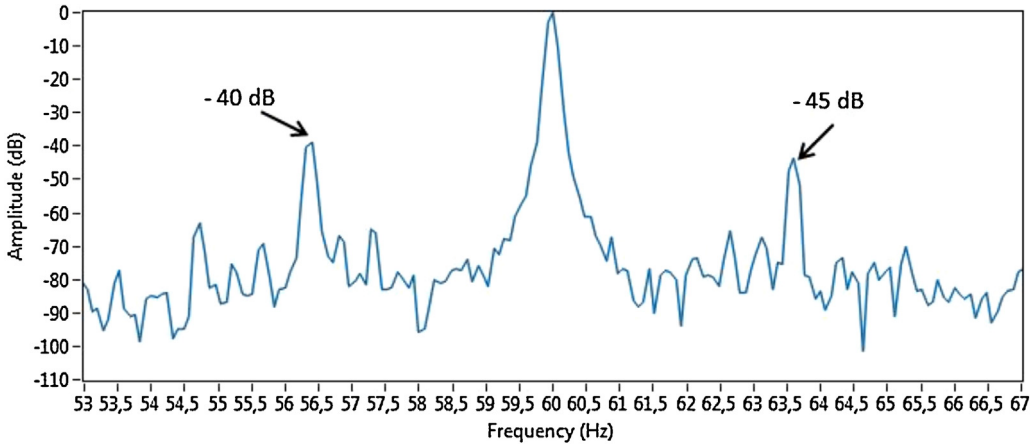

Fig. 6. Spectrum of current for loaded motor with one broken bar.

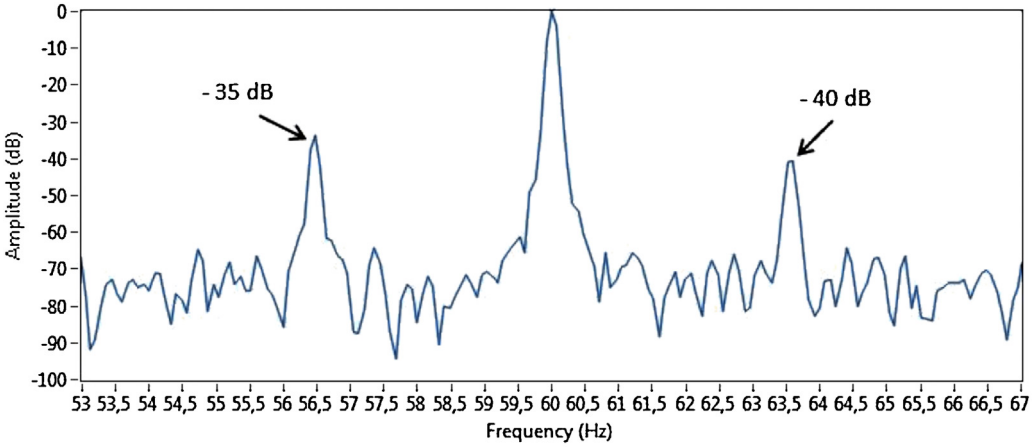

Fig. 7. Spectrum of current for loaded motor with two broken bar.

spectrum of stator current for a healthy motor at 90% of the rated load and motor speed is equal 1745 rpm. The amplitude of the f_{lsb} is 55 dB lower than the amplitude of the grid frequency (60 Hz) and amplitude of the f_{usb} is 70 dB lower.

Fig. 6 shows spectrum of stator current for one broken bar at 90% of the rated load and motor speed is equal 1745 rpm. The fault frequency components of the f_{lsb} (*lower side band*) is equal 56.33 Hz ($(1-2s)f_0$) and f_{usb} (*upper side band*) is equal 63.67 Hz ($(1+2s)f_0$) are analyzed. The amplitude of the f_{lsb} is 40 dB lower than the amplitude of the grid frequency and of the f_{usb} component is 45 dB lower.

Fig. 7 shows spectrum of stator current for two broken bars at 90% of the rated load and motor speed is equal 1745 rpm. The fault frequency components of the f_{lsb} (*lower side band*) is equal 56.40 Hz ($(1-2s)f_0$) and of the f_{usb} (*upper side band*) is equal 63.60 Hz ($(1+2s)f_0$) are analyzed. The amplitude of the f_{lsb} is 35 dB lower than the amplitude of the grid frequency and the amplitude of the f_{usb} is 40 dB lower.

Fig. 8 shows spectrum of stator current for three broken bars at 90% of the rated load and motor speed is equal 1745 rpm. The fault frequency components of the f_{lsb} (*lower side band*) is equal 57.30 Hz ($(1-2s)f_0$) and of the f_{usb} (*upper side band*) is equal 62.70 Hz ($(1+2s)f_0$) are analyzed. The amplitude of the f_{lsb} is 32 dB lower than the amplitude of the grid frequency and the amplitude of the f_{usb} is 32 dB lower.

In the test with 1, 2 and 3 broken rotor bars unloaded motor, at 0% of the nominal load (Fig. 9) the traditional FFT method analysis is not valid because the slip s is very low and the components of the right $(1+2s)f_0$ and left $(1-2s)f_0$ fault sideband overlap with the fundamental frequency f_0. Therefore, the resultant amplitude does not accurately indicate the motor condition on steady-state.

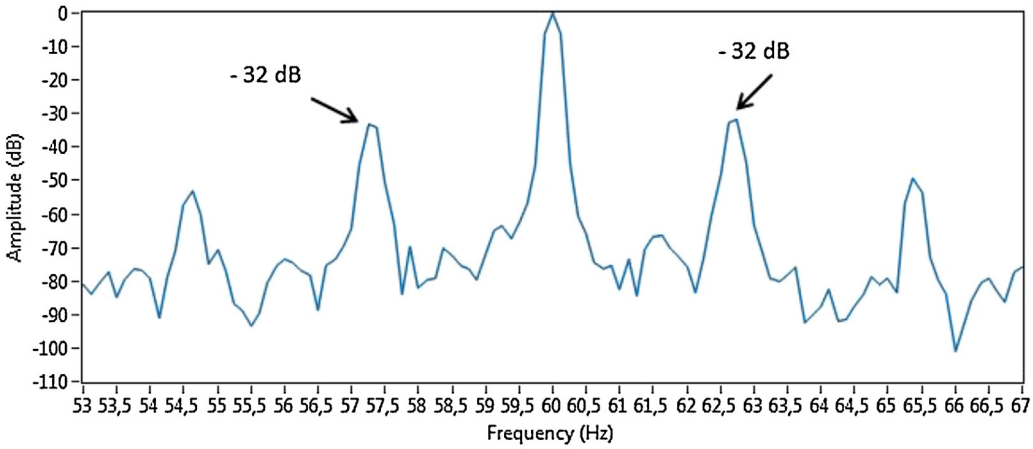

Fig. 8. Spectrum of current for loaded motor with three broken bar.

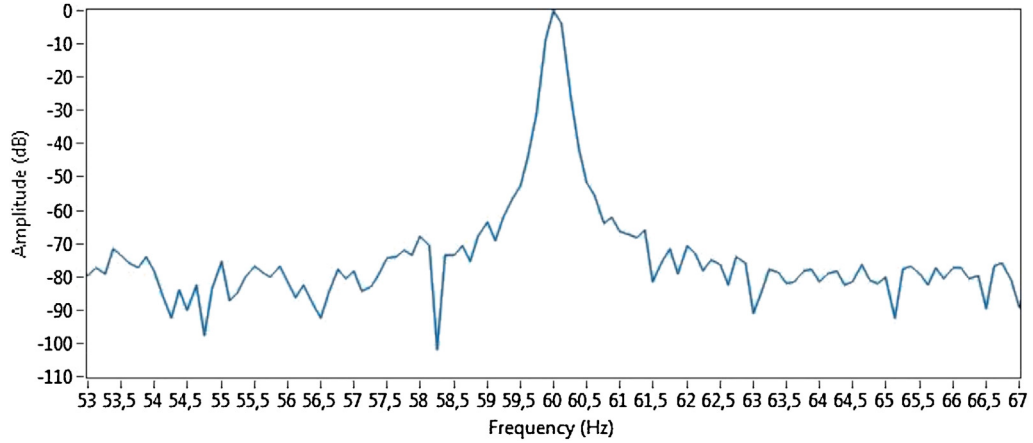

Fig. 9. Spectrum of current for unloaded motor with 1, 2 and 3 broken bars.

Table 1
Frequency bands for the high-level wavelet signals.

J0		F_s = 5000 Hz (0–2500 Hz) – N = 5000 samples		
J1	0–1250 Hz			
J2	0–625 Hz	625–1250 Hz		
J3	0–312.5 Hz	312.5–625 Hz		
J4	0–156.25 Hz	156.25–312.5 Hz		
J5	0–78.12 Hz	78.12–156.25 Hz		
J6	0–39.06 Hz	39.06–78.12 Hz		
J7	0–19.53 Hz	19.53–39.06 Hz	39.06–58.59 Hz	58.59–78.12 Hz
J8	0–9.76 Hz	9.76–19.53 Hz	19.53–29.3 Hz	29.3–39.06 Hz
	A8	D8	D7	D6

5.2. Experimental results with WT

The stator current of the induction motor was measured during the startup time of the motor, operation of the motor at 90% of the nominal load, for the different cases tested herein. The sampling frequency used for capturing the signal was 5000 samples/s. The approximation signal with level 8-decomposition was used in order to obtain the f_{lsb} (*lower side band*) harmonic. Table 1 shows the frequency bands corresponding to the high-order wavelet signals resulting from the analysis, according to the sampling rate (f_s = 5000 samples/s) used for tests.

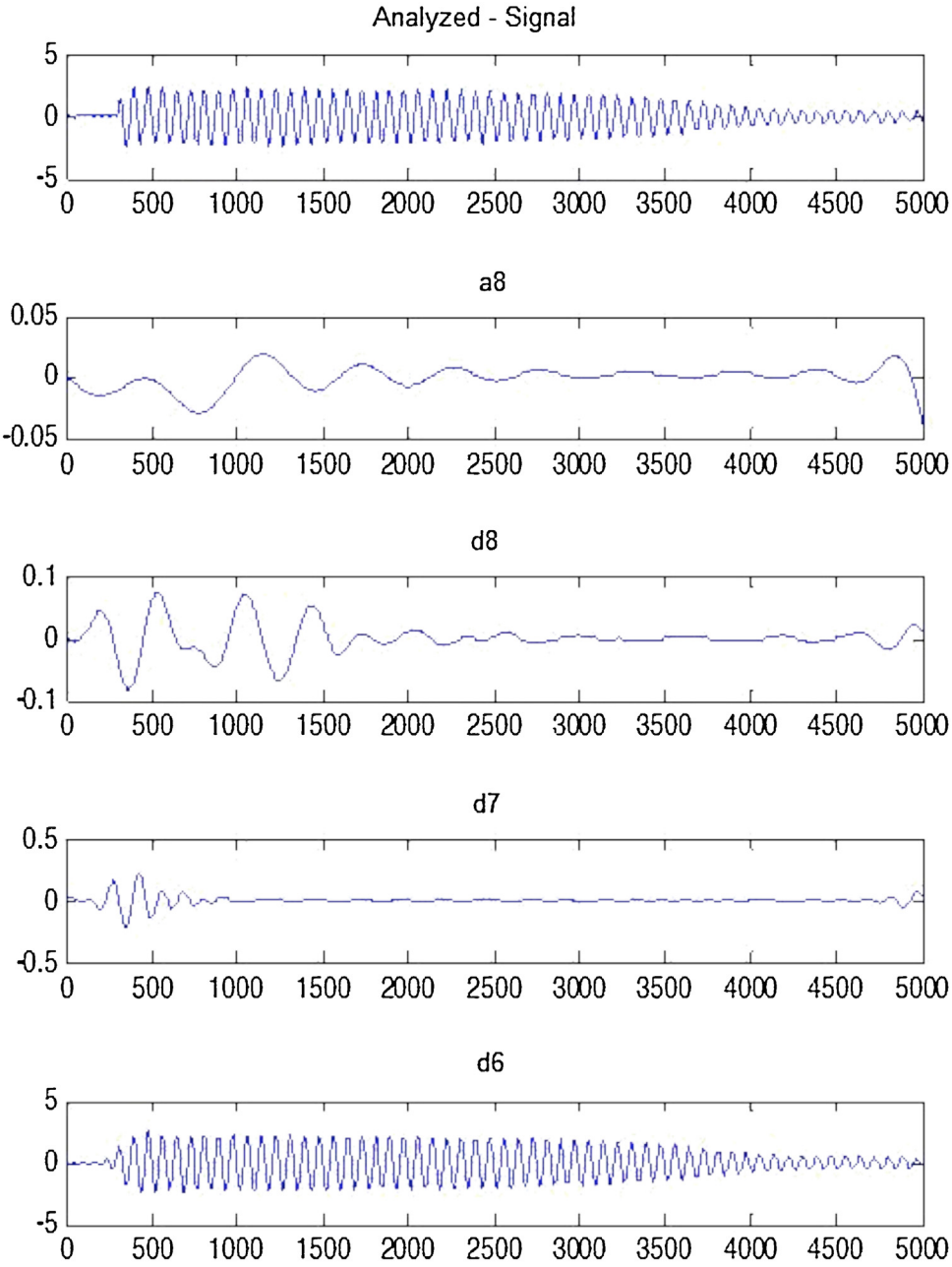

Fig. 10. 8 level DWT of the startup current for healthy motor under load.

The DWT of the stator current was obtained using the wavelet toolbox in MATLAB. Daubechies-44 mother wavelet was used for analysis of the current signal. Fig. 10 shows the primary current of the stator associated with the 8-level DWT of the startup current of a healthy motor under load. It can be seen that the upper level signal A8 (approximation), D8 and D7 (details) do not show any significant variation, apart from the initial oscillations that last only few cycles. From this, it can be concluded that the harmonic associated with broken bars is not present in this situation.

Fig. 11 displays the DWT analysis of the current of a loaded motor with two broken rotor bars. As shown in figure, a significant increase with respect to the healthy state appears in the energy of the upper level signals D8 and D7 (details). The oscillations in those signals are due to the evolution of the f_{lsb} (*lower side band*) component during the transient. These oscillations follow a sequence that is according to the frequency evolution of the f_{lsb} on FFT based

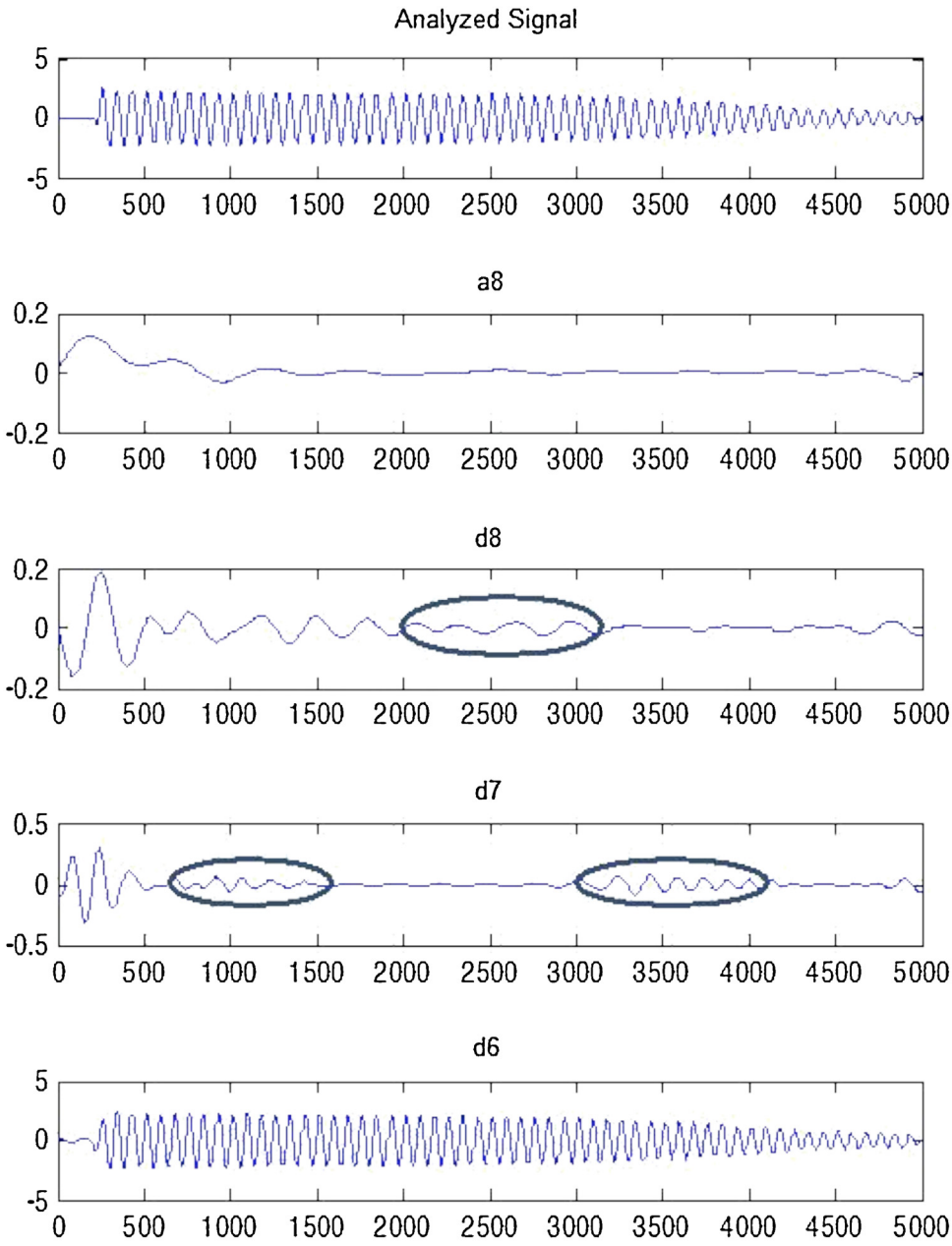

Fig. 11. 8 level DWT of the startup current for loaded motor with two broken rotor bars.

method. From this, it can be concluded that both methods inform about the presence of broken rotor bars in loaded machine.

Fig. 12 displays the DWT analysis of the current of an unloaded motor with three broken rotors bars. In this case, the application of the classical method, based on FFT analysis, is not valid, since the slip is very low and the sideband components overlap the supply frequency component. This makes very difficult the detection of the fault. Nevertheless, the upper order wavelet signals D8 and D7 details resulting from the DWT analysis of the startup current show a clear increase in their energy, if compared with the healthy state. In addition, their oscillations fit well with the f_{lsb} (*lower side band*) evolution described above. Thus, in this case, the information provided by the WT method can complement that given by the classical approach to reach a more accurate detection. This case is an example of the validity of the approach in a case when the classical FFT method is not suitable to be applied.

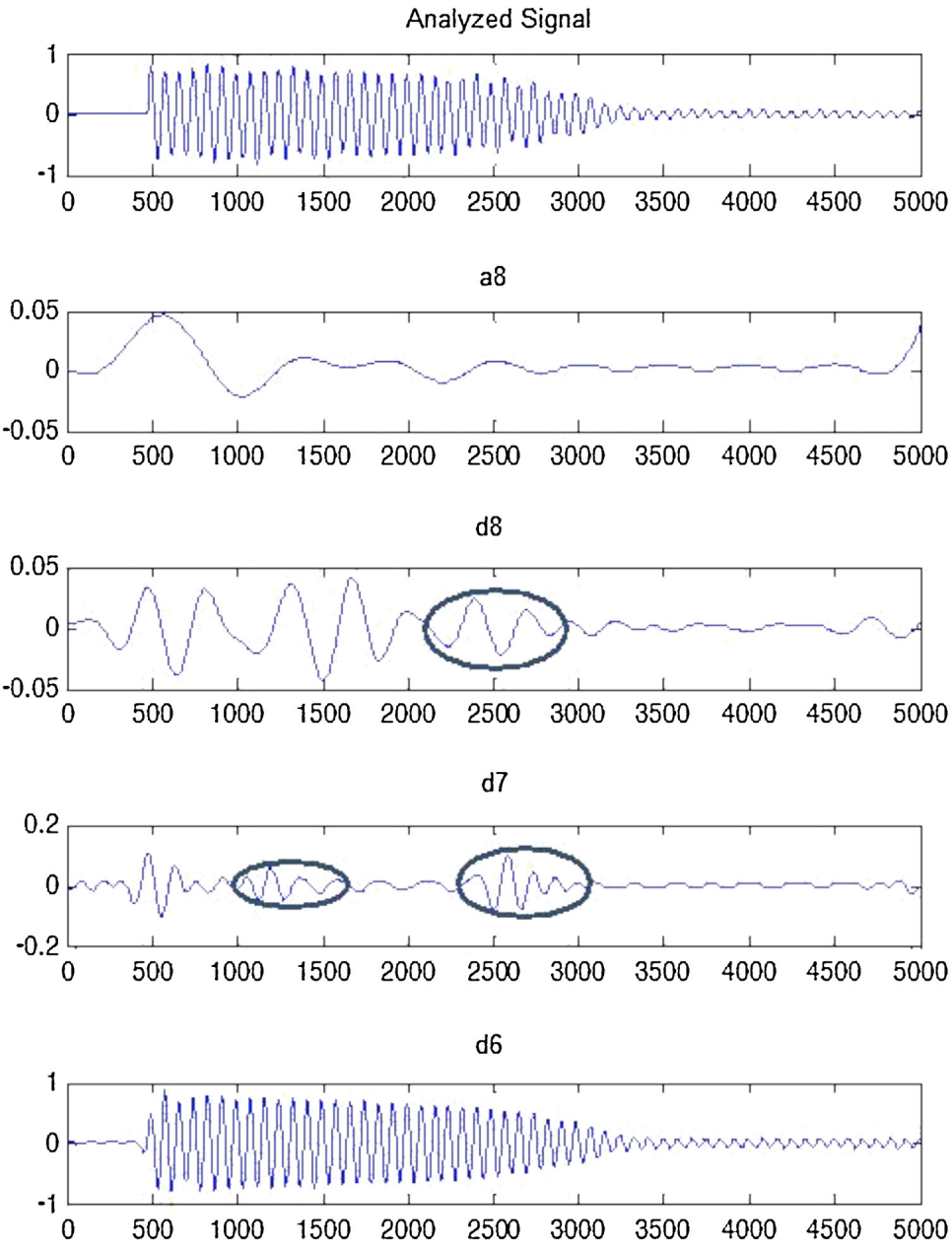

Fig. 12. 8 level DWT of the startup current for unloaded motor with three broken rotor bars.

6. Conclusions

This case study presents a comparison between two methods for the detection of rotor bar faults in induction cage motors, validated and optimized. The first case uses FFT method and allows for the classical detection of broken bars based on the application of the Fourier transform to the stator current of an induction motor running in the steady state. Fault detection is achieved by studying the two sideband components (lower and upper) that appear around the supply frequency component. This classical approach has important advantages such as simplicity of data acquisition systems and required software, as well as robustness, and it has provided quite satisfactory results hitherto. However, in some cases, unloaded induction motors, for instance, the slip s is very low and the sideband components practically overlap the supply frequency. This makes it difficult to detect their presence and use them for detection. The second case is based on the use of wavelet transform (WT). This technique allows for the decomposition of a signal into different frequency components, thus allowing for the study of each component separately in its corresponding scale. An advantage of wavelet transform during signal

decomposition is that it allows the user to analyze the information contained in a non-stationary signal at different time–frequency resolutions. The WT method can be considered as a complementation of traditional FFT method to non-stationary states. These detection methods can be considered as representative of new trend, to reach a diagnostic in some of the cases in which the conventional FFT method does not properly work.

References

[1] Kral C, Haumer A, Grabner C. Modeling and simulation of broken bars in squirrel cage induction machines. In: Proceedings of the World congress on engineering 2009, vol. I; 2009. p. 435–40.
[2] Kim YH, Youn YW, Hwang DH, Sun JH, Kang DS. High-resolution parameter estimation method to identify broken rotor bar faults in induction motors. IEEE Trans Ind Electron 2013;60:4103–17.
[3] Da Costa C, Mathias MH, Ramos P, Girão P. A new approach for real time fault detection in induction motors based on vibration measurement. In: Instrumentation and measurements technology conference (I2MTC), 2010 IEEE; 2010.p. 1164–8.
[4] Georgoulas G, Tsoumas IP, Daviu JAA, Alarcon VC. Automatic pattern identification based on the complex empirical mode decomposition of the startup current for detection of rotor asymmetries in asynchronous machines. IEEE Trans Ind Electron 2014;61(9):4937–46.
[5] Pu S, Zheng C, Yuriy V, Zoubir Z. A new detection of broken rotor bar fault extent in three phase squirrel cage induction motor. Mech Syst Signal Process 2013;42:388–403.
[6] Kaikaa MY, Hadjami M. Effects of the simultaneous of static eccentricity and broken rotor bars on the stator current of induction machine. IEEE Trans Ind Electron 2014;61(5):2452–63.
[7] Ebrahami BM, Faiz J, Lotfi-fard S, Pillay P. Novel indices for broken rotor bars fault detection in induction motors using wavelet transform. Mech Syst Signal Process 2012;30:131–45.
[8] Yan R, Gao RX, Chen X. Wavelet for fault detection of rotary machines: a review with application. Signal Process A 2014;96:1–15.
[9] He Q. Vibration signal classification by wavelet packet energy flow manifold learning. J Sound Vib 2013;332(7):1881–94.
[10] Antonino-Daviu J, Riera-Guasp M, Roger-Folch J, MartínezGiménez F, Peris A. Application and optimization of the discrete wavelet transform for the detection of broken rotor bars in induction machines. Appl Comput Harmon Anal 2006;21(September):268–79.
[11] Shao R, Hu W, Wang Y, Qi X. The fault feature extraction and classification of gear using principal component analysis and kernel principal component analysis based on the wavelet packet transform. Measurement 2014;54:118–32.
[12] Briz F, Degnert MW, Garcia P, Bragado D. Broken rotor bar detection in line-fed induction machines using complex wavelet analysis of startup transients. IEEE Trans Ind Appl 2008;44(May/Jun (3)):760–8.
[13] Mohanty AR, Kar C. Fault detection in a multistage gearbox by demodulation of motor current waveform. IEEE Trans Ind Electron 2006;53(August (4)):1285–97.
[14] Bin GF, Gao JJ, Li XJ, Dhillon BS. Early fault detection of rotating machinery based on wavelet packets – empirical mode decomposition feature extraction and neural network. Mech Syst Signal Process 2012;27:696–711.
[15] Rajagopalan S, Aller JM, Restrepo JA, Habetler TG, Harley RG. Analytic-wavelet-ridge-based detection of dynamic eccentricity in brushless direct current (BLDC) motors functioning under dynamic operating conditions. IEEE Trans Ind Electron 2007;54(June (3)):1410–9.
[16] Ye Z, Wu B, Sadeghian A. Current signature analysis of induction motor mechanical faults by wavelet packet decomposition. IEEE Trans Ind Electron 2003;50(December (6)):1217–28.
[17] Cusido J, Romeral L, Ortega JA, Rosero JA, Garcia Espinosa A. Fault detection in induction machines using power spectral density in wavelet decomposition. IEEE Trans Ind Electron 2008;55(February (2)):633–43.
[18] Supangat R, Ertugrul N, Soong WL, Gray DA, Hansen C, Grieger J. Detection of broken rotor bars in induction motor using starting-current analysis and effects of loading. Proc Inst Elect Eng Elect Power Appl 2006;153(November (6)):848–55.
[19] Ordaz-Moreno A, Romero-Troncoso R, Vite-frías JA, RivieraGillen J, García-Pérez A. Automatic online diagnostic algorithm for broken-bar detection on induction motors based on discrete wavelet transform for FPGA implementation. IEEE Trans Ind Electron 2008;55(May (5)):2193–200.
[20] Riera-Guasp M, Antonino-Daviu J, Roger-Folch J, Molina MP. The use of the wavelet approximation signal as a tool for the detection and quantification of rotor bar failures. IEEE Trans Ind Appl 2008;44(May/Jun (3)):716–26.
[21] Antonino-Daviu J, Riera-Guasp M, Roger-Folch J, Pilar Molina Palomares M. Validation of a new method for the detection of rotor bar failures via wavelet transform in industrial induction machines. IEEE Trans Ind Appl 2006;42(July/August (4)):990–6.